Forward dijets at the LHC as a probe for saturation using a new model for impact parameter dependent TMDs

Federico M. Deganutti, Soeren Schlichting, Christophe Royon

The University of Kansas,The University of Bielefeld

Low-x , Leros (Greece)

fedeganutti@ku.edu

Sep 5, 2023

* Very forward jets at LHC
* Small-x (I)TMD framework
* Azimuthal correlation in pp and pA in "naive" scaling approx.
* Compute TMDs from dipole scattering amplitudes fitted to DIS Hera data
* How to reintroduce Impact-Parameter dependence?
  - Borrowing ideas from AAMQS and IPSat
  - Fixing model parameters using the proton case as reference
  - Model predictions deviate significantly from naive expectations
* Conclusions

$p-p$ and $p-A$ in dilute-dense kinematics

Forward (same hemisphere) di-jets *to* dilute-dense asymmetry: (dilute) proton projectile probes (**dense**) proton or nucleus target at small-x

$$\text{Process}: \quad p + \mathbf{A} \to j_1 + j_2 + X$$

(when X is small) $\mathbf{k} = \mathbf{p}_{j_1} + \mathbf{p}_{j_2} \Leftrightarrow k_t$:
di-jet momentum imbalance $\Leftrightarrow$ gluon (in target) initial transverse momentum
need **small-x TMD** to describe **target**

usual collinear PDF to describe probe

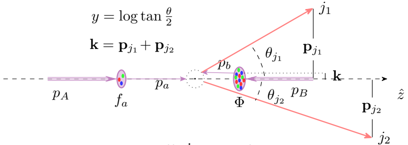

scattering geometry

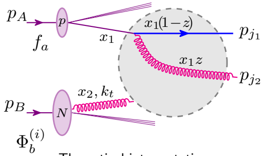

Theoretical interpretation

Linear (BFKL) or non-linear (saturation) small-x QCD dynamics depending on relative size of k_t and the saturation scale $Q_s(x)$
All gluon TMDs coincide in the large k_t limit into the unintegrated gluon distribution

Improved-TMDs[Marquet et all:1503.03421]:
smooth interpolation between H-E and TMD

k_t *v.s.* Q_s discriminates between regimes

$$\left.\begin{array}{ll} Q_s \sim k_t; & \text{TMD fact.} \\ Q_s \ll k_t; & \text{High-Energy fact.} \end{array}\right\} \Rightarrow \quad p_j \gg Q_s, \text{ any } k_t; \ \text{I-TMD}$$

Cross section:

$$\frac{d\sigma}{dJ_1 dJ_2} = \frac{\alpha_s}{(x_1 x_2 s)^2} x_1 f_f(x_1) H^{(i)}_{\rm ITMD}(P_t, k_t)\Phi^{(i)}(x_2, k_t) \begin{cases} H^{(i)}_{\rm TMD}(P_t)\Phi^{(i)}(x_2, k_t) \\ |\mathcal{M}_{\rm HE}|^2 g(x_2, k_t) \end{cases}$$

Azimuthal angle distribution

Azimuthal (de)correlation of very forward di-jets as proxy for hadron internal dynamics at small x and transverse momentum $k_t \sim Q_s$

- Sensitive to saturation at small azimuthal angles $\Delta\phi_j \Leftrightarrow$ small $k_t = |\mathbf{k}|$

ITMD applied to azimuthal correlation of forward di-jets in pp vs pA[Marquet et all.:1607:03121]

- LHC kinematics: $\sqrt{s} = 8.16$ TeV, $p_j > 20$ GeV, $3.5 < y < 4.5$ forward region
- Nuclear modif. fact.: $R_{pPb} = \frac{\mathrm{d}\sigma^{p+Pb}}{\mathrm{d}\Delta\phi} \Big/ A \frac{\mathrm{d}\sigma^{p+p}}{\mathrm{d}\Delta\phi}$
- Nucleus case in "naive" scaling approx.: $\frac{1}{R^2} \to \frac{A}{R_A^2} \Rightarrow \left(Q_s^A\right)^2 = A^{1/3} Q_s^2(x)$

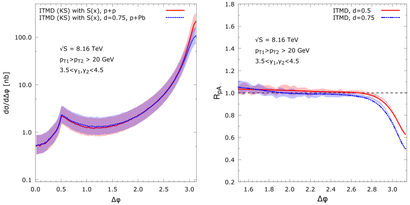

Larger saturation scale in nuclei causes the nuclear modification factor to drop towards the back-to-back limit

The nuclear TMDs "stops rising" at larger $k_t \sim Q_s^A$ while the proton TMDs did not reach saturation yet

- TMDs were calculated in gaussian-approximation and large N_c limit: $\Rightarrow$

ALL TMD as derivatives of dipole-amplitude $F = F\left(\left\{\partial_i, \partial_j N(r,x)\right\}\right)$

- Evolution provided by the KS solution to BK eq.
- Missing Sudakov-logarithms

Dipole amplitude from HERA data

Deep-inelastic Scattering (DIS) represents the most direct way of probing the saturation regimes
Precise measurement of nuclear distributions down to very small x at HERA
Dipole picture: tot. cross-section *factorizes* into (1) photon wave function Ψ and impact parameter averaged (twice the imaginary part of) dipole-target scattering amplitude

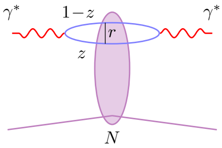

dipole-shockwave interaction schematic

$$\sigma_{T,L}(x, Q^2) = 2 \int \mathrm{d}z \int \mathrm{d}^2\mathbf{b}\, \mathrm{d}^2\mathbf{r} \left|\Psi^{\gamma}_{L,T}(Q^2, \mathbf{r})\right|^2 \mathcal{N}(\mathbf{r}, \mathbf{b}, x)$$

$$\Rightarrow \sigma_p \int \mathrm{d}z \int \mathrm{d}^2\mathbf{r} \left|\Psi^{\gamma}_{L,T}(Q^2, \mathbf{r})\right|^2 \mathcal{N}(\mathbf{r}, x)$$

TMDs can be computed from $\mathcal{N}(\mathbf{r}, x)$ or $\mathcal{N}(\mathbf{r}, \mathbf{b}, x)$

AAMQS[A non-linear QCD analysis of new HERA data at small-x:1012.4408]

- BK evolution equation with running coupling corrections (rcBK): Excellent accuracy
- No need full complexity of JIMWLK eq.?
- But, heavy-flavors with ad-hoc normalization

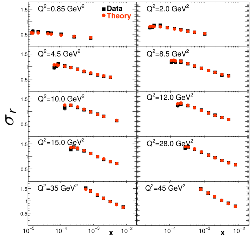

Unperturbative initial condition (McLerran-Venugopalan) MV^{γ}-model
exponentiation follows from eikonal approximation

$$\mathcal{N}^{MV^{\gamma}}(r, x0 = 0.01) = 1 - exp\left[-\frac{(rQ_{s0})^{2\gamma}}{4}\log(\frac{1}{r\Lambda} + e)\right], \quad \begin{cases} Q_{s0} \text{ sat. scale} \\ \gamma \text{ anomalous dim.} \\ \Lambda \text{ IR cut}-\text{off} \end{cases}$$

AAMQS fit will be the basis for our model

Impact parameter dependence

Rigorous treatment requires solution of b-dependent rcBK equation (or JIMWLK) but is complicated: Diffusion, confinement

Simple attempt: DGLAP based IPsat model[hep-ph/0304189]:

Other attempts: b-CGC

Nuclear transverse thickness $T(b)$ "at exponent" of Glauber-Mueller dipole amplitude:

$$\mathcal{N}^{\rm IPsat}(r,x,b) = 1 - exp\left[-\frac{\pi^2}{2N_c} r^2 \alpha_s(\mu^2) xg(x,\mu^2) T(\mathrm{b})\right]$$

Features: unitary, good fit to F2 struct. func., straight forward generalization to nuclei

- Valid when DGLAP logs dominates over BFKL logs
- Could be improved in the small-x region

We prosose hybrid model: (1) rcBK x-evolved MV^{γ} dipole amplitude *a la* AAMQS; (2) impact parameter dependence restored *a la* IPSat

(1) Fit a MV^{γ} inspired formula at each value of x

$$\mathcal{N}(\hat{r},x) = 1 - exp(G(Q_s(x), r, \gamma(x), \ldots))$$

$$G(\tilde{r} = r/r_S(x), x) = -\frac{(\tilde{r}Q_{s0}(x))^{2\gamma(x)}}{4}\log\left(\frac{1}{\tilde{r}\Lambda(x)} + ee_C(x)\right)$$

$$Q_s = 1/r_S :\rightarrow G(r = r_S) = \frac{1}{4}$$

(2) Promote impact-parameter dependence in fitted formulae

$$\mathcal{N}\left(\{G(Q_s, \mathbf{b}, r, \gamma, \ldots)\}\right) \rightarrow \mathcal{N}\left(\{T_A(b)G(Q_s, r, \gamma, \ldots)\}\right)$$

Comparable $\mathcal{N}(x,r)$ *v.s.* $\mathcal{N}(x,r,\mathbf{b})$ accuracy of F_2 predictions

$$F_2(x,Q^2) = \frac{Q^2}{4\pi^2\alpha_{em}}\left[\sigma_T(x,Q^2) + \sigma_L(x,Q^2)\right]$$

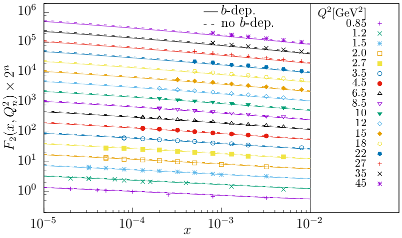

Model parameters and Nuclear thickness

How to reintroduce the IP dependence back into the b-averaged dipole fits?

$$S_\perp \mathcal{N}(\{G(r,x)\}) \to \int \mathrm{d}^2\mathbf{b}\mathcal{N}(\{G(r,x,b)\}) = \begin{cases} S_\perp \frac{\eta}{\sigma} \int \mathrm{d}^2\mathbf{b}\,(1 - exp[\sigma G(r,x) T(\mathbf{b})])\,, & T(b) > T_{\min} \\ 0, & \text{otherwise} \end{cases}$$

Model Parameters: $\{\eta, \sigma, T_{\min}\}$

- $T_{\min} > 0$ cut-off necessary for finite result $\Leftrightarrow$ shockwave picture valid at large densities

Transverse thickness: T_p, T_A

- Proton: gaussian shape $T_p(\mathbf{b}) = \frac{exp(-b^2/(2B_G))}{2\pi B_G}$
- Nucleus: sum of each proton and neutron $T_p = T_n$ gaussian thickness

$$T_A(\mathbf{b}) = \sum_{i=1}^{A} T_{p/n}(\mathbf{b}_i - \mathbf{b})$$

- Nucleon positions $\{\mathbf{b}_1, \ldots, \mathbf{b}_i\}$ are generated stochastically via Glauber MC event-per-event tuned to Wood-Saxon distribution

$$\rho_{\mathrm{W.S.}}(r = \sqrt{\underline{x}^2}; R, a) = \frac{\rho_0}{1 + \exp r - Ra}\,,$$

$\mathbf{b}_i$ is the transverse projection of i-th nucleon 3-dim position $\underline{x}_i$

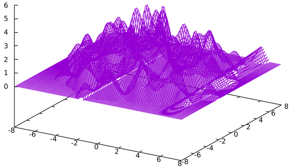

Lead thickness with $T_{\min}$ cut-off

	A	R[fm]	a[fm]
p	1	$\sqrt{B_G} = 4$ GeV	/
O	16	2.61	0.51
Xe	129	5.36	0.57
Pb	207	6.62	0.55

Crucial Model assumption (unavoidable starting from b-averaged fits)
$G_{\mathbf{x},\mathbf{y}}(x) = G_{\frac{\mathbf{b}+\mathbf{r}}{2},\frac{\mathbf{b}-\mathbf{r}}{2}}(x) \simeq G_{|\mathbf{r}|}(x)\tilde{T}_A(\mathbf{b})$

Matching b-dep. and b-indep. proton TMDs

All gluon Transverse Momentum Distributions (TMDs) F can be calculated as correlator of Wilson-lines from the dipole density G

We take the proton case as reference and match the model predictions for the TMDs $F(x, r, \mathbf{b})$ to the corresponding known impact parameter averaged ones $\overline{F}(x, r)$

$$\overline{F}(x,r) \stackrel{?}{=} \langle F(x,r,\mathbf{b})\rangle \equiv \frac{\eta}{\sigma}\int_{T_{\min}} \mathrm{d}^2\mathbf{b}\, F(\{\sigma T_p(\mathbf{b}) G(\mathbf{r},x)\})$$

$$\frac{\overline{F}^{(1)}_{qg}}{S_\perp} = \left[G^{(1,1)}(r,x) - G^{(1,0)}(r,x)G^{(0,1)}(r,x)\right] e^{G^{(0,0)}(r,x)}\,, \qquad G^{i,j}(r) = -\partial_i\partial_j G(r)$$

$$\frac{\langle F^{(1)}_{qg}(b)\rangle}{S_\perp} = \int_{T_{\min}} d^2b \left[\eta T_p(b) G^{(1,1)}(r,x) - \sigma T_p^2(b) G^{(1,0)}(r,x) G^{(0,1)}(r,x)\right] e^{\sigma T_p(b) G^{(0,0)}(r,x)}$$

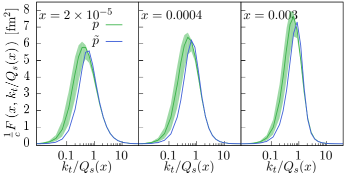

Fourier transform of dipole TMDs $\mathcal{F}_{qg}$

The values of $\eta = 1/\mathcal{A}_p, \sigma = 1/\mathcal{T}_p$ are fixed matching the large-k_t tails (where $exp(\sigma G T) \simeq 1$) of Fourier-transformed TMDs.

$$\mathcal{A}_p = \int_{T(b)\geq T_{\min}} d^2b\; T_p(b), \qquad \mathcal{A}_p\mathcal{T}_p = \int_{T(b)\geq T_{\min}} d^2b\; T_p^2(b)$$

Reasonable cut-off value: density at twice the gaussian width $T_{\min} = T(2\sqrt{B_g}) \simeq 0.14\,\mathrm{fm}^{-2}$

Estimate model error by varying $T_{\min} \pm 50\%$

η, σ depend on $T_{\min}$ but not on A!

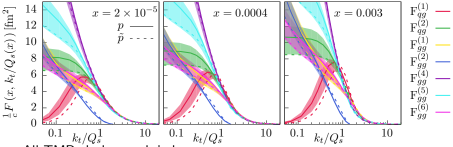

All TMDs b-dep. vs b-indep.

Nuclear TMDs

Once the model parameters are fixed, nuclear TMDs are calculated by swapping $T_p \Leftrightarrow T_A$

In plots the TMDs are rescaled

- Along the $\hat{x}$-axis by $Q_s^A \equiv \sqrt{\sigma \mathcal{T}_A} Q_s$
- along the $\hat{y}$-axis by $\rho_\perp^A \equiv \frac{S_\perp^A}{S_\perp^p} = \frac{\mathcal{A}_A}{\mathcal{A}_p} \frac{\mathcal{T}_A}{\mathcal{T}_p}$ along the $\hat{y}$-axis

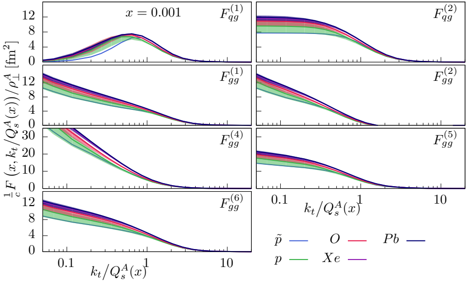

All TMDs rescaled along $\hat{x}$ and $\hat{y}$ axes

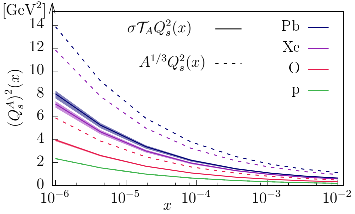

Model v.s Naive Saturation scales (squared) as func. of x

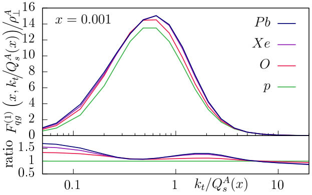

Rescaled dipole TMDs for nuclei and ratio to proton

Error bands indicate model uncertainty.

Model scaling works well at large k_t

Model scaling vs naive scaling

Compare model calculated nuclear TMDs for p, O, Xe, Pb to naive scaling:

$$F^{\mathrm{model}}(x, k_t, A) \simeq \rho_\perp^A \overline{F}^p(x, k_t/[\sigma \mathcal{T}_A Q_s^p])$$

v.s.

$$F^{\mathrm{naive}}(x, k_t, A) \equiv A^{2/3} \overline{F}^{\tilde{p}}(x, k_t/[A^{1/6} Q_s])$$

Results:

- Model predicts higher and broader TMD peaks
- Fair agreement at large k_t
- Ratio profile will show up in Nuclear modification factor

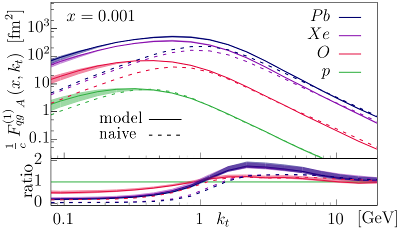

Model *v.s.* Naive dipole TMDs for nuclei and respective ratios to protons as func. of k_t

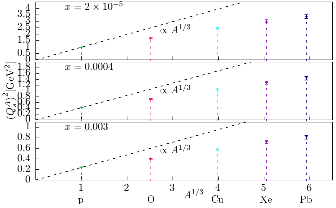

$(Q_s^A)^2$ (colored bars) *v.s.* $A^{1/3} Q_s^2$ (dashed) as func. of A

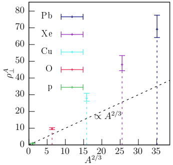

Normalization factor $\rho_\perp^A$ (colored bars) *v.s.* $A^{2/3}$ (dashed line) as func. of A

Weaker A-scaling in saturation scale but stronger in TMD magnitude

Forward dijets in CMS and Castor/Focal kinematics

Observables: (1) Azimuthal di-jet decorrelation; (2) Nuclear Modification factor

$$\frac{\mathrm{d}\sigma}{\mathrm{d}J_1\mathrm{d}J_2} = \frac{\alpha_s}{(x_1 x_2 s)^2} x_1 f_f(x_1) H^{(i)}_{\mathrm{ITMD}}(P_t, k_t)\Phi^{(i)}(x_2, k_t)$$

$$\frac{\mathrm{d}\sigma}{\mathrm{d}\Delta\phi_{j_{12}}} = \int\Big[\prod_{n=1,2}\mathrm{d}^2\mathbf{p}_{j_n}\mathrm{d}y_{j_n}\Big]\frac{\mathrm{d}\sigma}{\mathrm{d}J_1\mathrm{d}J_2}\theta\left(\Delta\phi_{j_{12}} - (\phi_{j_1} - \phi_{j_2})\right) \qquad R_{pA} = \frac{\mathrm{d}\sigma^A}{\mathrm{d}\Delta\phi_{j_{12}}}\Big/ A\frac{\mathrm{d}\sigma^p}{\mathrm{d}\Delta\phi_{j_{12}}}$$

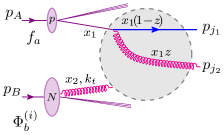

Theoretical picture

Cross sections in very forward Castor/Focal kinematics

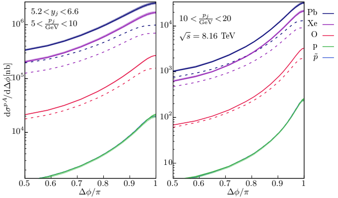

- Peaked towards "back-to-back"
- More pronounced for p and softer/forward jets
- Model (solid) deviates significantly from naive scaling (dashed)

Cross sections in Forward CMS kinematics

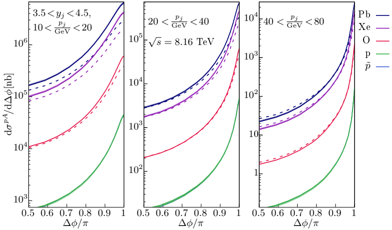

Forward dijets in CMS and Castor/Focal kinematics

Observables: (1) Azimuthal di-jet decorrelation; (2) Nuclear Modification factor

$$\frac{d\sigma}{dJ_1 dJ_2} = \frac{\alpha_s}{(x_1 x_2 s)^2} x_1 f_f(x_1) H^{(i)}_{\rm ITMD}(P_t, k_t)\Phi^{(i)}(x_2, k_t)$$

$$\frac{d\sigma}{d\Delta\phi_{j_{12}}} = \int\Big[\prod_{n=1,2} d^2\mathbf{p}_{j_n} dy_{j_n}\Big] \frac{d\sigma}{dJ_1 dJ_2}\theta\left(\Delta\phi_{j_{12}} - (\phi_{j_1} - \phi_{j_2})\right) \qquad R_{pA} = \frac{d\sigma^A}{d\Delta\phi_{j_{12}}} \Big/ A\frac{d\sigma^p}{d\Delta\phi_{j_{12}}}$$

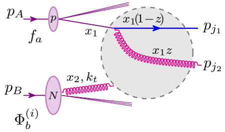

Theoretical picture

Nuclear mod. fac. in very forward Castor/Focal kinematics

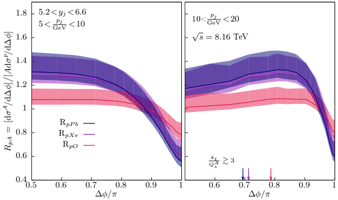

Nuclear mod. fac. in Forward CMS kinematics

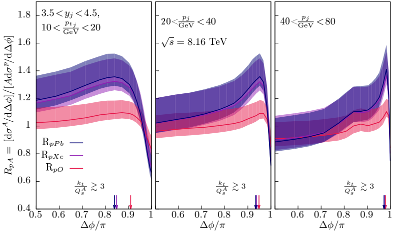

- *Xe*, *Pb* develop a "knee" before dropping towards "back-to-back"
- Saturation region (from knee to $\Delta\phi = \pi$) squeezed for central and hard jets
- Colored arrows point at $\Delta\phi^*$ separating TMDs sampled at: left $k_t/Q_s^A > 3$; right $k_t/Q_s^A > 3$.

Model v.s. Naive for $p - Pb$

Model and Naive dipole TMDs

$$F^{\text{model}}(x, k_t, A) \simeq \rho_\perp^A \, \overline{F}^p(x, k_t/[\sigma \mathcal{T}_A Q_s^p])$$

v.s.

$$F^{\text{naive}}(x, k_t, A) \equiv A^{2/3} \overline{F}^{\tilde{p}}(x, k_t/[A^{1/6} Q_s])$$

Model *v.s.* Naive dipole TMDs for nuclei and respective ratios to protons as func. of k_t

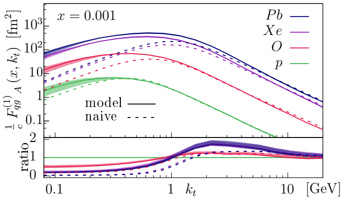

Nuclear mod. fac. in very forward Castor/Focal kinematics

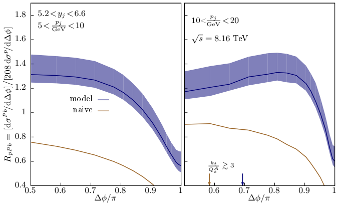

Nuclear mod. fac. in Forward CMS kinematics

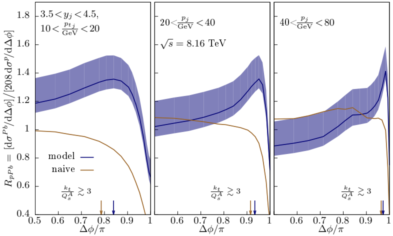

- Evident disagreement between model and naive predictions: especially when saturation effects are stronger
- Knee not seen on naive predictions

Conclusions

* Model for Impact-Parameter dep. TMDs
* Hybrid setup:
  - Inclusive dipole amplitude from AAMQS fit to HERA
  - *b*-dependence *a la* IPsat
  - Model parameter fixed using proton as benchmark
* Results:
  - Model predicts weaker scaling in nuclear saturation energy
  - Broader and larger TMDs then naive case
  - "Knee" region at intermediate angles before induced suppression due to saturation

Back-up

Why is R_{pA} not reaching unity in $\Delta\phi \to 0$ limit?

At small $\Delta\phi$ corresponds large k_t/Q_s^A where $F(k_t, x, A) \sim S_\perp^A (k_t/Q_s^A)^{2\lambda}$

λ depends weakly on x and A; $\pm 10\%$ in A and x range; $\lambda \simeq 0.85 - 1.12$

Suppose we neglect A dependence in λ:

$\sigma^A \propto F(k_t, x, A) \sim S_\perp^A (k_t/Q_s^A)^\lambda \propto S_\perp^A (Q_s^A)^{2\lambda}$

$R_{pA} \sim S_\perp^A (Q_s^A)^{2\lambda} \Big/ A S_\perp^p (Q_s^p)^{2\lambda}$

Model: $R_{pA} \sim \frac{\mathcal{A}_A}{A\mathcal{A}_p} \left(\frac{\mathcal{T}_p}{\mathcal{T}_A}\right)^{2(\lambda-1)}$

Naive: $R_{pA} \sim \frac{A^{2/3}}{A} \left(A^{1/6}\right)^{2(\lambda-1)}$

But even discarding the A dependence $\lambda = \lambda(x)$!

TMDs calculation

1. Gluon TMDs

Starting point of our discussion is the operator definition of the TMDs in the small-x limit, where the relevant TMDs for di-jet production take the form (c.f. arXiv:1608.02577v2)

$$\frac{g^2(2\pi)^3}{4S_\perp}F_{qg}^{(1)}(\mathbf{k}) = \int d^2(\mathbf{x}-\mathbf{y})\, e^{-i\mathbf{k}(\mathbf{x}-\mathbf{y})}\,\mathrm{Tr}\Big[\left(\partial_i^{\mathbf{x}}V_{\mathbf{x}}^\dagger\right)\left(\partial_i^{\mathbf{y}}V_{\mathbf{y}}\right)\Big]\,, \tag{1}$$

$$\frac{g^2(2\pi)^3}{4S_\perp}F_{qg}^{(2)}(\mathbf{k}) = \frac{-1}{N_c}\int d^2(\mathbf{x}-\mathbf{y})\, e^{-i\mathbf{k}(\mathbf{x}-\mathbf{y})}\,\mathrm{Tr}\Big[\left(\partial_i^{\mathbf{x}}V_{\mathbf{x}}\right)V_{\mathbf{y}}^\dagger\left(\partial_i^{\mathbf{y}}V_{\mathbf{y}}\right)V_{\mathbf{x}}^\dagger\Big]\mathrm{Tr}\Big[V_{\mathbf{y}}V_{\mathbf{x}}^\dagger\Big]\,, \tag{2}$$

for the qg channel and for the gg channel

$$\frac{g^2(2\pi)^3}{4S_\perp}F_{gg}^{(1)}(\mathbf{k}) = \frac{+1}{N_c}\int d^2(\mathbf{x}-\mathbf{y})\, e^{-i\mathbf{k}(\mathbf{x}-\mathbf{y})}\,\mathrm{Tr}\Big[\left(\partial_i^{\mathbf{x}}V_{\mathbf{x}}^\dagger\right)\left(\partial_i^{\mathbf{y}}V_{\mathbf{y}}\right)\Big]\mathrm{Tr}\Big[V_{\mathbf{x}}V_{\mathbf{y}}^\dagger\Big]\,, \tag{3}$$

$$\frac{g^2(2\pi)^3}{4S_\perp}F_{gg}^{(2)}(\mathbf{k}) = \frac{-1}{N_c}\int d^2(\mathbf{x}-\mathbf{y})\, e^{-i\mathbf{k}(\mathbf{x}-\mathbf{y})}\,\mathrm{Tr}\Big[\left(\partial_i^{\mathbf{x}}V_{\mathbf{x}}\right)V_{\mathbf{y}}^\dagger\Big]\mathrm{Tr}\Big[\left(\partial_i^{\mathbf{y}}V_{\mathbf{y}}\right)V_{\mathbf{x}}^\dagger\Big]\,, \tag{4}$$

$$\frac{g^2(2\pi)^3}{4S_\perp}F_{gg}^{(3)}(\mathbf{k}) = -\int d^2(\mathbf{x}-\mathbf{y})\, e^{-i\mathbf{k}(\mathbf{x}-\mathbf{y})}\,\mathrm{Tr}\Big[\left(\partial_i^{\mathbf{x}}V_{\mathbf{x}}\right)V_{\mathbf{y}}^\dagger\left(\partial_i^{\mathbf{y}}V_{\mathbf{y}}\right)V_{\mathbf{x}}^\dagger\Big]\,, \tag{5}$$

$$\frac{g^2(2\pi)^3}{4S_\perp}F_{gg}^{(4)}(\mathbf{k}) = -\int d^2(\mathbf{x}-\mathbf{y})\, e^{-i\mathbf{k}(\mathbf{x}-\mathbf{y})}\,\mathrm{Tr}\Big[\left(\partial_i^{\mathbf{x}}V_{\mathbf{x}}\right)V_{\mathbf{x}}^\dagger\left(\partial_i^{\mathbf{y}}V_{\mathbf{y}}\right)V_{\mathbf{y}}^\dagger\Big]\,, \tag{6}$$

$$\frac{g^2(2\pi)^3}{4S_\perp}F_{gg}^{(5)}(\mathbf{k}) = -\int d^2(\mathbf{x}-\mathbf{y})\, e^{-i\mathbf{k}(\mathbf{x}-\mathbf{y})}\,\mathrm{Tr}\Big[\left(\partial_i^{\mathbf{x}}V_{\mathbf{x}}\right)V_{\mathbf{y}}^\dagger V_{\mathbf{x}}V_{\mathbf{y}}^\dagger\left(\partial_i^{\mathbf{y}}V_{\mathbf{y}}\right)V_{\mathbf{x}}^\dagger V_{\mathbf{y}}V_{\mathbf{x}}^\dagger\Big]\,, \tag{7}$$

$$\frac{g^2(2\pi)^3}{4S_\perp}F_{gg}^{(6)}(\mathbf{k}) = \frac{-1}{N_c^2}\int d^2(\mathbf{x}-\mathbf{y})\, e^{-i\mathbf{k}(\mathbf{x}-\mathbf{y})}\,\mathrm{Tr}\Big[\left(\partial_i^{\mathbf{x}}V_{\mathbf{x}}\right)V_{\mathbf{y}}^\dagger\left(\partial_i^{\mathbf{y}}V_{\mathbf{y}}\right)V_{\mathbf{x}}^\dagger\Big]\mathrm{Tr}\Big[V_{\mathbf{x}}V_{\mathbf{y}}^\dagger\Big]\mathrm{Tr}\Big[V_{\mathbf{y}}V_{\mathbf{x}}^\dagger\Big]\,, \tag{8}$$

From Wilson line ensemble in Gaussian approximation. Large N_c and Finite N_c